Proc. Natl. Acad. Sci. USA
Vol. 90, pp. 10429–10433, November 1993
Biochemistry

Multiple oligomeric states regulate the DNA binding of helix–loop–helix peptides

(protein–protein interactions/protein–DNA interactions/electrophoretic mobility shift assay/circular dichroism/sedimentation equilibrium)

ROBERT FAIRMAN*†, RITA K. BERAN-STEED*, SPENCER J. ANTHONY-CAHILL*‡, JAMES D. LEAR*, WALTER F. STAFFORD III§, WILLIAM F. DEGRADO*¶, PAMELA A. BENFIELD*, AND STEPHEN L. BRENNER*¶

*DuPont Merck Pharmaceutical Co., Experimental Station, P.O. Box 80328, Wilmington, DE 19880-0328; and ‡Department of Muscle Research, Boston Biomedical Research Institute, 20 Staniford Street, Boston, MA 02114

Communicated by Donald M. Crothers, July 6, 1993

ABSTRACT **To study the protein–protein interactions that allow Id, a negative regulator of cell differentiation, to inhibit the DNA-binding activities of MyoD and E47, we have synthesized peptides corresponding to the helix–loop–helix domains of MyoD, E47, and Id. We show that Id preferentially inhibits the sequence-specific DNA-binding activity of MyoD, a muscle-specific protein, as compared to E47, a more ubiquitous protein. The Id helix–loop–helix domain itself forms stable tetramers, and its inhibitory activity arises from the formation of a heterotetrameric structure with MyoD. The formation of this higher order complex provides a general mechanism by which inhibitory proteins can generate sufficient interaction free energy to overcome the large DNA-binding free energy of dimeric DNA-binding proteins.**

Id (inhibitor of DNA binding) is a protein that negatively regulates gene expression via direct protein–protein interaction to prevent DNA binding of other helix–loop–helix (HLH)-containing proteins (1). Id belongs to a rapidly growing family of DNA-binding proteins related by amino acid sequences that are predicted to fold into a common structural domain, the HLH (for recent reviews, see refs. 2–4). This domain mediates homo- and heterooligomerization of multiple transcription factors, in a similar fashion to the leucine zipper class of DNA-binding proteins, providing a higher order program of gene regulation via interactions between differentially expressed polypeptides. In some cases the leucine zipper and HLH motifs are both present in the same protein, such as in the protooncogene-encoded protein c-Myc and its partner, Max (5).

In HLH-containing transcription regulators, a lysine- and arginine-rich basic region is typically found N-terminal to the HLH region and is essential for DNA binding (6). The HLH motif provides a dimerization interface that positions two DNA-binding domains to confer high-affinity site-specific binding to DNA sequences with approximate inversional symmetry. Experimental evidence for dimerization comes from electrophoretic mobility shift studies of the binding of E47 and MyoD to DNA (6, 7). Three similar models that describe the structure of basic region–HLH (bHLH) dimers bound to DNA have been proposed (8–10). More recently the cocrystal structure of Max, a bHLH/leucine zipper protein, bound to DNA has been determined (11). Heterodimer formation is an important regulatory mechanism for HLH proteins: activation of myogenesis by MyoD requires the action of heterodimers of MyoD, a muscle-specific protein, and E47 or E12 (12), two ubiquitously expressed proteins also involved in the regulation of immunoglobulin gene expression (6, 13).

The publication costs of this article were defrayed in part by page charge payment. This article must therefore be hereby marked "*advertisement*" in accordance with 18 U.S.C. §1734 solely to indicate this fact.

Since the discovery of the HLH motif, a new subclass of proteins has been found that can inhibit the function of HLH DNA-binding proteins by heterooligomer formation (1, 14–18). These proteins inhibit site-specific DNA binding because they lack a functional basic domain and can form heterooligomers with proteins such as MyoD and E47. Id, one member of this subclass, can inhibit DNA binding of a truncated form of MyoD containing only the basic and HLH domains, indicating that the interaction of the HLH domains of both proteins is sufficient for inhibition (1).

A simple mechanism for inhibition would involve forming a heterodimer between Id and the target protein, thus producing a dimer with only one functional DNA-binding domain. However, such a mechanism will work only if the Id protein is present in great excess over the DNA-binding protein and/or the interaction between Id and the DNA-binding protein is much more favorable than dimerization and DNA binding of the target protein.

The finding that several HLH proteins—for example, MyoD (8) and myogenin (19)—form tetramers in solution suggests an alternate mechanism for inhibition involving the formation of heterotetramers between Id and the DNA-binding proteins. A heterotetramer might be able to compete more effectively with DNA binding because its formation involves not only the favorable monomer–monomer interactions that stabilize the dimers but also interactions between the dimers, which can compensate for the loss in favorable DNA–protein interactions.

In this work, we determine which of the two models, heterodimer or heterotetramer formation, best describes the mechanism by which Id inhibits the binding of HLH proteins to DNA, and we assess the minimal sequence requirements for this inhibition. To achieve these goals, we synthesized peptides representing the HLH motifs of MyoD, E47, and Id and then studied their DNA-binding and oligomerization equilibria using electrophoretic mobility shift assays (EMSA), circular dichroism (CD) spectroscopy, and sedimentation equilibrium (SE) ultracentrifugation. We propose that the observed tetrameric forms of HLH proteins serve a critical biological role in regulating gene transcription by a sensitive concentration-dependent switch, which buffers the amount of the active (hetero-) dimeric transcription factors available to bind DNA.

MATERIALS AND METHODS

Peptides were synthesized and purified as discussed (8). Purity and peptide identity were verified by electrospray

Abbreviations: HLH, helix–loop–helix; SE, sedimentation equilibrium; EMSA, electrophoretic mobility shift assay(s); bHLH, basic region–HLH.

†Present address: Department of Macromolecular Structure, Bristol–Myers Squibb, P.O. Box 4000, Princeton, NJ 08543-4000.
‡Present address: Somatogen, Inc., 5797 Central Avenue, Boulder, CO 80301.
¶To whom reprint requests should be addressed.

	Basic region	Helix 1	Loop	Helix 2
MyoD bHLH:	NADRRKAATMRERRR	LSKVNEAFETLKRST	SSNPNQRLP	KVEILRNAIRYIEGLQALLRDQ
MyoD S-S:	NADRRKAATMRERRR	LSKVNEAFETLKRST	SSNPNQRLP	KVEILRNAIRYIEGLQALLRAC
E47 bHLH:	LEEKDLRDRERRMANNARERVR	VRDINEAFRELGRMS	QMHLKSDKAQT	KLLILQQAVQVILGLEQQVRERG
Id aHLH:	TRLPALLDEQQVNVL	LYDMNGSYSRLKELV	PTLPQNRKVS	KVEILQHVIDYIRDLQLELNSE
Id HLH:		LYDMNGSYSRLKELV	PTLPQNRKVS	KVEILQHVIDYIRDLQLELNSE
MyoD-Id:	NADRRKAATMRERRR	LYDMNGSYSRLKELV	PTLPQNRKVS	KVEILQHVIDYIRDLQLELNSE

FIG. 1. Peptide sequences used in this work.

mass spectrometry, amino acid analysis, analytical HPLC, and, in some cases, N-terminal amino acid sequence analysis and capillary zone electrophoresis. The peptides used in this study were >90% pure except for the MyoD peptide used in the MyoD/Id CD experiment (>75% pure). The peptide concentration was checked by tyrosine absorbance (20) or by quantitative amino acid analysis. The peptide sequences used in this work are shown in Fig. 1.

The DNA-binding assays are a modification of a method described by Benezra *et al.* (1). The DNA is a 25-bp oligonucleotide whose sequence is GATCCCCCCAACACCTGCTGCCTGA and contains the right E box (underlined) from the mouse muscle creatine kinase enhancer (21).

Samples for CD analysis were typically prepared in 0.15 M NaCl/0.01 M Mops, pH 7.5. Measurements were made using an Aviv 62DS CD spectropolarimeter at 25°C. The peptide concentration-dependence data were fit by nonlinear least-squares methods to various equilibrium schemes using a PC version of the program MLAB (Civilised Software, Bethesda, MD) (22). We used numerical methods for solving linked equilibrium problems similar to those described (23).

SE experiments were carried out on a Beckman Instruments model E analytical ultracentrifuge equipped with a real-time video-based data acquisition system and Rayleigh optics (24). Details and methods of data analysis were as described (25–27).

RESULTS

EMSA Analysis of the Interactions Between Id, MyoD, and E47. A 47-aa fragment of Id containing just the HLH domain (Id HLH) is an effective inhibitor of MyoD homodimer and MyoD–E47 heterodimer DNA binding, as judged by EMSA analysis (Fig. 2 *A* and *C*). However, Id is a 10- to 100-fold weaker inhibitor of DNA binding by the E47 homodimer (Fig. 2*B*). The Id HLH peptide shows no intrinsic DNA-binding activity in the concentration range reported here (data not shown).

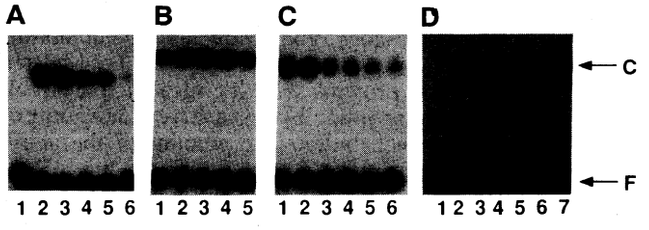

FIG. 2. Inhibition of DNA binding by Id HLH. (*A*) Inhibition of MyoD bHLH peptide. Lane 1, free DNA; lanes 2–6, 5.5 μM MyoD plus 0, 0.7, 6, 14, and 28 μM Id HLH peptide, respectively. (*B*) Inhibition of E47 bHLH peptide. Lanes 1–5, 4.7 μM E47 plus 0, 0.7, 6, 14, and 28 μM Id HLH peptide, respectively. (*C*) Inhibition of MyoD–E47 heterodimers. Lanes 1–6, 2.7 μM MyoD bHLH peptide and 2.3 μM E47 bHLH peptide plus 0, 0.7, 6, 14, 28, and 57 μM Id HLH peptide, respectively. (*D*) Inhibition of MyoD S-S peptide. Lane 1, free DNA; lanes 2–7, 5.5 μM MyoD S-S peptide plus 0, 0.1, 7, 14, 29, and 43 μM Id HLH peptide, respectively. F, free DNA; C, peptide–DNA complexes.

The basic sequence N-terminal to the HLH domain in DNA-binding proteins of this class is helical when bound to DNA (8, 11). In contrast, the same region in Id has a predicted net charge of −1 at neutral pH and contains helix-breaking residues. A 62-residue Id peptide (aHLH) containing this sequence was synthesized (Fig. 1), and it was found that this acidic N-terminal domain of Id plays little role in the inhibition of DNA binding, with the exception of a slight enhancement of inhibition of E47 binding to DNA (data not shown).

To determine if Id inhibits MyoD DNA binding by interacting directly with the fully folded homodimer of MyoD, we combined the Id HLH peptide with a disulfide cross-linked derivative of the MyoD peptide via a cysteine introduced at the C-terminal end of helix 2 (Fig. 1; MyoD S-S). This cross-linked MyoD species binds to DNA with the same specificity as the corresponding reduced, non-cross-linked peptide (8). Fig. 1*D* shows that, in contrast to the native MyoD peptide, there is no inhibition, even at an Id-to-MyoD molar ratio of 20:1, suggesting that the disulfide bridge, while not interfering with DNA binding, is incompatible with the formation of a MyoD–Id complex.

We also asked if the HLH domain of Id is capable of supporting site-specific binding to DNA. A hybrid was prepared in which the basic domain of MyoD was fused onto the HLH domain of Id (Fig. 1; MyoD-Id). The DNA-binding activity of this peptide is compared to MyoD DNA-binding in Fig. 3. Although this MyoD–Id fusion peptide does show strong affinity and some specificity for binding to the rat muscle creatine kinase enhancer site, smaller differences are seen between the equilibrium constants for specific and nonspecific DNA binding. Analysis of the Id HLH peptide (described below) suggests that the extent of nonspecific binding exhibited by the MyoD–Id fusion is related to the strong preference for Id to form a tetramer, which presum-

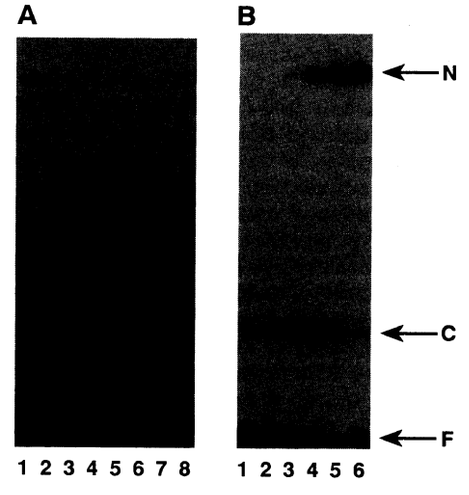

FIG. 3. DNA binding of the fusion peptide. F, free DNA; C, peptide–DNA complexes; N, nonspecific peptide–DNA complexes. (*A*) MyoD bHLH binding to DNA. Lane 1, free DNA; lanes 2–8, DNA plus 1.1, 2.2, 3.3, 4.4, 5.5, 11, and 22 μM MyoD bHLH peptide, respectively. (*B*) MyoD-Id binding to DNA. Lanes 1–6, DNA plus 4.4, 5.5, 11, 16, 22, 44 μM MyoD–Id peptide.

ably does not juxtapose the basic domains properly for sequence-specific DNA binding.

Oligomerization States of MyoD and E47. To determine the oligomerization states of Id with the MyoD and E47 peptides, it is first necessary to analyze the oligomerization states of MyoD and E47 alone or in combination. Sedimentation equilibrium (SE) studies from Laue *et al.* (28) have shown that the HLH domain of E47 forms homodimers and that this fragment also heterodimerizes with MyoD HLH peptides in the absence of DNA. This finding is supported by our analysis of the line widths in NMR spectra of E47 (R.F., unpublished results). On the other hand, SE analysis of the MyoD bHLH peptide (data not shown) confirmed the findings by Starovasnik *et al.* (29) that this peptide exists as an equilibrium between monomers, dimers, and tetramers in the concentration range from 10 μM to 200 μM.

To quantitate the oligomerization of the peptides, we take advantage of the fact that the monomeric peptides have disordered conformations while the dimeric and tetrameric forms of the peptides have considerable α-helical content (8). Thus, the transition from monomers to oligomers can be monitored by measuring the intensity of the CD band at 222 nm ($[\theta]_{222}$), allowing the determination of dissociation constants for the MyoD and E47 peptides individually and for the MyoD/E47 peptide mixture.

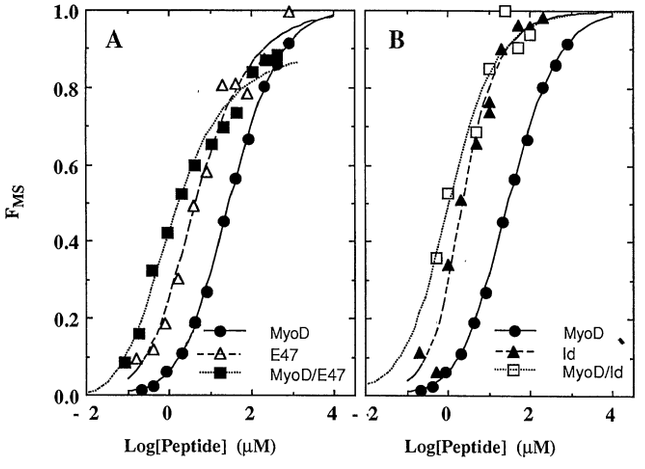

FIG. 4. Binding isotherms for the monomer–oligomer equilibria for MyoD, E47, and MyoD/E47 HLH peptides (*A*) and MyoD, Id, and MyoD–Id HLH peptides (*B*). (*A*) The peptide concentration of the heterodimer is expressed in terms of the MyoD peptide concentration. The MyoD/E47 mixture contains a mixed population of homomeric and heteromeric species, so a linked equilibrium approach is necessary to evaluate the heteromeric parameters. (The fitted curve for MyoD/E47 is calculated by using the homomeric plus the heteromeric parameters from Table 1 as constants.) This explains the apparent plateau of the fitted curve for MyoD/E47 falling below 1.0. F_{MS} is defined as the fraction of the maximum CD signal expected at infinite peptide concentration for the experiment. At sufficiently high concentrations, the E47–MyoD heterodimer ($[\theta]_{max}$ = 15.0) will disappear as the MyoD forms tetramers ($[\theta]_{max}$ = 22.0). (*B*) The MyoD data and fitted curve are taken from *A*, and the Id data are taken from Fig. 5*A*. Because of the extreme stability of the MyoD–Id complex, a complete isotherm was not measurable. The association isotherm for the MyoD–Id heteromeric complex was measured at pH 6.5 rather than pH 7.5, due to problems with solubility. pH effects on stability are minimal in the range encompassing 6.5–7.5 (data not shown). The dissociation constants calculated for the Id homomeric species (as described in Fig. 5) and the MyoD–Id heteromeric species thus represent an upper limit to their expected values under standard conditions. The CD data for the MyoD–Id complex were manually fit with linked equilibrium schemes in a similar fashion to the data for MyoD/E47; however, an additional term was added describing a heterotetramer species, since a heterodimer model did not adequately describe the apparent highly cooperative transition.

Fig. 4*A* illustrates the fraction of the maximal CD signal as a function of the concentration of the E47 and MyoD peptides and a 1:1 mixture of the two species. The data show two interesting features. First, the transition from unstructured monomers to helical oligomers occurs in the high nanomolar to low micromolar concentration range. Thus, at lower protein concentrations, binding to DNA can only occur by paying the additional entropic cost of bringing together and folding the two monomeric proteins. Second, the MyoD–E47 complex shows the greatest stability, and MyoD shows the least stability with E47 showing intermediate stability as judged by the midpoints of the isotherms.

The dissociation constant for the dimer of E47 (Table 1) was obtained from nonlinear least-squares curve fitting of the peptide concentration dependence of $[\theta]_{222}$ using Eq. **1**:

$$D \underset{}{\overset{K_{1,2}}{\rightleftharpoons}} 2M, \qquad K_{1,2} = \frac{[M]^2}{[D]} \qquad [1]$$

where M and D are the monomer and dimer forms of E47 and $K_{1,2}$ is the dissociation constant. The parameters required for fitting were $K_{1,2}$ and $[\theta]_{222}$ for the monomer ($[\theta]_{min}$) and dimer ($[\theta]_{max}$) forms.

The analysis of the data for MyoD was somewhat more complex because this peptide forms tetramers. We assume a monomer–dimer–tetramer scheme for this peptide because MyoD binds to DNA as a dimer and the homologous E47 peptide forms stable dimers in solution. Thus, dimers are likely to be stable intermediates in the tetramerization of the MyoD peptide according to Eq. **2**:

$$T \underset{}{\overset{K_{2,4}}{\rightleftharpoons}} 2D \underset{}{\overset{(K_{1,2})^2}{\rightleftharpoons}} 4M, \qquad K_{2,4} = \frac{[D]^2}{[T]}, \qquad [2]$$

where M, D, and T are the monomer, dimer, and tetramer forms, respectively, and $K_{1,2}$ and $K_{2,4}$ are the dissociation

Table 1. Dissociation constants for HLH oligomers

Peptide	$K_{1,2}$, μM	$K_{2,4}$, μM	$[\theta]_{max}$, deg·cm^2·dmol^{-1}	$[\theta]_{min}$, deg·cm^2·dmol^{-1}
MyoD*	31.2	338	−21,200	−5100
E47†	4.5	—	−16,200	−1400
Id* (25°C)	5.3	0.36	−14,500	−1900
Id* (60°C)	21.6	21.1	−13,900	−1800
MyoD/E47†	0.72	—	−14,900	−3300‡
MyoD/Id*	0.7	0.01	−22,000	−3500‡

*The data for MyoD, Id, and MyoD/Id were fitted using a monomer–dimer–tetramer equilibrium scheme (see Fig. 5 legend for general comments). Since MyoD forms weakly associated tetramers, $K_{2,4}$ is ill-defined, as judged by the sum of squared residuals, with the greatest uncertainty lying in the upper bounds. However, $K_{2,4}$ for MyoD is in reasonable agreement with sedimentation equilibrium analysis (where $K_{2,4} \approx 200$ μM). For Id, two minima were found for the sum-of-squared residuals corresponding to the sets ($K_{1,2}$, $K_{2,4}$) = (5.3, 0.36) and (15, 0.03). Significant excursions away from these values produced poorer fits. More importantly, both sets of values for Id produced the reported higher degree of hetero- vs. homotetramer formation in the fitting of the MyoD/Id mixed equilibria experiments. Finally, the heteromeric $K_{1,2}$ and $K_{2,4}$ values given above for MyoD/E47 and MyoD/Id proved to be relatively insensitive to test excursions from the best-fit values for the homomeric $K_{1,2}$ and $K_{2,4}$ values. Further error analysis of the heteromeric $K_{1,2}$ and $K_{2,4}$ values for the MyoD/Id data unequivocally demonstrate the qualitative conclusion that $K_{2,4}$ must be significantly smaller than $K_{1,2}$.

†The data for E47 and MyoD/E47 were fitted using a dimerization equilibrium scheme with standard deviations (95% confidence) in $K_{1,2}$, $[\theta]_{max}$, and $[\theta]_{min}$ for E47 of ±1.4, ±500, and ±800 and for MyoD/E47 of ±0.34, ±500, and ±800.

‡The value of $[\theta]_{min}$ for the 1:1 mixtures is an average of the experimentally determined signal for each monomer.

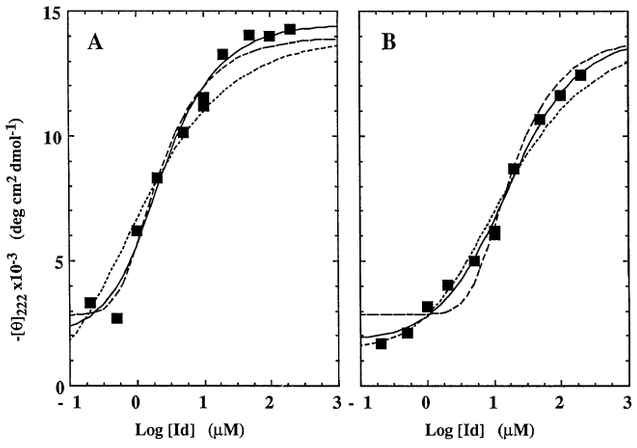

FIG. 5. Binding isotherms for Id HLH at 25°C (*A*) and 60°C (*B*) fit with monomer–dimer (short dashes), monomer–tetramer (long dashes), and monomer–dimer–tetramer (solid line) equilibrium schemes. Id HLH was measured in 0.45 M urea/0.01 M Mops, pH 7.5, because of solubility problems. We found, in separate experiments, that this concentration of urea had no appreciable effect on the structural stability of the Id peptide, and the unfolding is fully reversible. The parameters derived from curve fitting ($K_{1,2}$, $K_{2,4}$, $[\theta]_{max}$, and $[\theta]_{min}$) are reported in Table 1. The need to introduce the additional parameter, $K_{2,4}$, for the monomer–dimer–tetramer equilibrium scheme results in significant uncertainty in $K_{1,2}$ and $K_{2,4}$. The product, $(K_{1,2})^2(K_{2,4})$, defines the overall monomer–tetramer equilibrium; hence, $K_{1,2}$ and $K_{2,4}$ are difficult to determine independently. Further computational analysis revealed that the quality of the fit remains good within an order of magnitude variation in the ratio of $K_{1,2}$ and $K_{2,4}$, where the product, $(K_{1,2})^2(K_{2,4})$, is held constant. A similar computational approach was used to analyze the monomer–dimer–tetramer equilibrium for MyoD (see footnote * in Table 1).

constants for the dimers and tetramers, respectively. Several limiting cases for this equilibrium can be envisioned: if the formation of dimers from two monomers is more favorable than the formation of tetramers from two dimers ($K_{1,2} \ll K_{2,4}$) and given that the helix content of the dimers and tetramers is similar, then the curve will take on the appearance of a monomer–dimer equilibrium. On the other hand, if the dimerization of monomers is weak relative to the formation of tetramers from dimers ($K_{1,2} \gg K_{2,4}$), then the system behaves as a cooperative monomer–tetramer equilibrium ($4M \rightleftharpoons T$). Finally, if the two dissociation constants are similar, then they both need to be considered to model the isotherms. The last case holds for the MyoD data, which are fit best by a monomer–dimer–tetramer equilibrium with dissociation constants for the dimers and tetramers that are within an order of magnitude of one another (Fig. 4 and Table 1).

A rigorous analysis of the MyoD/E47 mixture requires a linked equilibrium approach because of the formation of both homo- and heterooligomeric dimers and tetramers. In this case, the dissociation constant for MyoD–E47 heterodimer formation was easily determined by nonlinear least-squares methods because the homomeric monomer–dimer and dimer–tetramer dissociation constants had already been independently determined. As anticipated from visual inspection of the curves in Fig. 4*A*, the dissociation constant for heterodimer formation is significantly smaller than that for homodimerization of either MyoD or E47 (Table 1).

Association of Id with MyoD. We next probed the role of Id as a selective inhibitor. SE showed that the Id HLH peptide forms stable tetramers in the range from 20 to 300 μM (data not shown). Because this peptide dissociates only at very low peptide concentrations, it is difficult to measure to high precision complete peptide oligomerization isotherms by the CD method at room temperature under standard conditions (Fig. 5*A*). However, we found that the Id HLH peptide completely dissociated at experimentally accessible peptide concentrations at 60°C (Fig. 5*B*), allowing very accurate measurements to be made under conditions where the peptide was predominantly monomeric (60°C) or predominantly self-associated (25°C). These CD experiments also clearly demonstrate that the data for Id are best described by a monomer–dimer–tetramer scheme (using the form of Eq. 2).

Fig. 4*B* compares the CD concentration dependence for MyoD (from Fig. 4*A*), Id (from Fig. 5*A*), and a 1:1 mixture of Id and MyoD at 25°C. Two observations are made for the MyoD and Id homomeric data: the Id HLH peptide shows greater stability than MyoD, and it also shows a steeper slope in the transition zone, illustrating greater cooperativity for formation of the Id tetramer as compared to the MyoD tetramer (see Table 1 for the appropriate dissociation constants). As in the case with the E47/MyoD mixture, the transition midpoint for the MyoD/Id mixture is shifted to lower concentrations relative to the MyoD and Id transition midpoints. We could not use CD to determine a dissociation constant for the E47–Id heterooligomer because the heteromeric association is weaker than their homomeric associations.

DISCUSSION

This paper shows that the tetrameric forms of HLH peptides are important to the regulation of the DNA-binding activity of this class of transcription factors. Full-length MyoD can form oligomers as well (29), suggesting that the observations for the HLH domains alone are relevant to the full-length proteins. Further support comes from studies on HLH proteins (19, 31), where tetrameric forms were identified. Tetramers could play a role in buffering transcriptional regulation by controlling the protein concentration range over which active dimers are available to bind DNA (31).

A major finding of this paper is that HLH domains from different proteins have varying abilities to form dimers and tetramers, and this phenomenon may act as an important regulator of activity. The E47 HLH domain forms dimers over a wide concentration range because the dimer association is much stronger than the association of two dimers to form tetramers. For the MyoD HLH domain, dimers and tetramers have similar association constants and, as a consequence, regulate DNA-binding, because tetramers of MyoD do not bind to DNA with sequence specificity and tetramer formation limits the available pool of dimers. The Id HLH domain forms stable tetramers in a highly cooperative process resulting in a low concentration of dimer intermediates. Most significantly, the Id HLH has an even stronger cooperativity and affinity for heterotetramerization with the MyoD bHLH peptide. Thus, Id effectively eliminates the ability of MyoD to bind DNA via the formation of the mixed tetramer. To illustrate the value of forming such heterotetramers, it is instructive to consider the ability of Id to inhibit MyoD DNA-binding utilizing either heterodimers or heterotetramers (Fig. 6) using the dissociation constants given in Table 1. Given a dissociation constant of 0.01 μM for a MyoD–DNA complex, Fig. 6*A* shows the amount of Id required to dissociate the MyoD from DNA by forming a heterodimer versus a heterotetramer. As expected, the difference in the models is more dramatic when MyoD is in greater excess over DNA (Fig. 6*B*), where the strength of the individual protein–protein interactions largely determines the distribution of oligomeric species.

This analysis suggests an elegant mechanism for inhibition of DNA binding by using concentrations of Id that need not be considerably greater than that for MyoD. The necessary interaction free energy is simply obtained from higher order oligomer formation. The finding that the Id–MyoD heterotet-

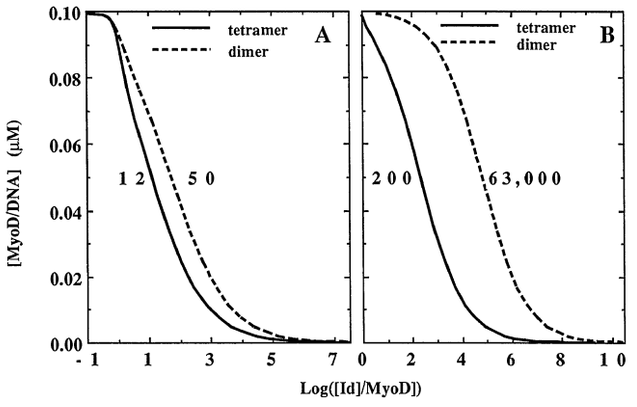

FIG. 6. Mathematical models describing the effects of Id on MyoD–DNA complex formation using either 10 μM MyoD (*A*) or 100 μM MyoD (*B*). Conditions chosen for the modeling were 0.1 μM DNA, K_d^{DNA} = 0.01 μM. The K_d^{DNA} is estimated from our EMSA analyses. The other dissociation constants required are taken from Table 1. The MyoD-to-Id molar ratios at the transition midpoints are reported next to their corresponding curves. The general qualitative conclusions of this model were resistant to the absolute values of the MyoD concentration, the DNA concentration, and K_d^{DNA} over at least two orders of magnitude.

ramer complex does not bind DNA would suggest that the tertiary structure of MyoD in the complex is different than in the active DNA-binding dimer. This conclusion is further supported by the lack of DNA-binding inhibition of the crosslinked MyoD dimer (Fig. 2*D*). If the tertiary structure of the heterotetramer is significantly different from the DNA-binding dimer structure, then Id must recognize different specificity determinants in its interaction with MyoD. It will be important to estimate the effective concentrations of both protein and site-specific DNA *in vivo* to fully understand the details of this form of regulation of gene expression.

A second finding of this paper is a clear demonstration that the Id HLH domain is sufficient to inhibit the binding of MyoD bHLH homodimers and MyoD–E47 bHLH heterodimers to DNA. These results are consistent with the results seen for the full-length proteins (1) in which it was shown that full-length Id protein could inhibit the binding to DNA of both MyoD and truncations of MyoD containing only its bHLH domain.

The Id HLH peptide is less efficient at inhibiting the binding of E47 homodimers to DNA. However, results from other laboratories (1, 14) have shown, using EMSA experiments, that Id is a more potent inhibitor of E47 than of MyoD. A reconciliation of these observations may come from mutagenesis experiments (32) showing that the efficient inhibition of E47 DNA binding is lost when only the HLH domain of Id is used. Clearly, other, more distal domains in these proteins must also influence Id's ability to inhibit DNA binding of E47. The data in this paper should provide a useful basis for further investigations into the role of other domains in regulating the DNA-binding activities of these proteins.

Finally, comparison of relative affinities for the DNA-bound forms of MyoD and E47 shows the following order of stability (30):

$$(MyoD)_2\text{–DNA} < (E47)_2\text{–DNA} < (MyoD\text{–}E47)\text{–DNA}.$$

The ordering of the stabilities of the protein–DNA complexes (30) is the same as the order of stabilities of the peptide dimers. In fact, the DNA-binding preference appears to be largely dictated by the dimer stabilities. Interestingly, the most stable dimer, the MyoD–E47 heterodimer, is the DNA-binding species that activates myogenesis (12).

We thank Sharon A. Jackson for peptide synthesis, George Koukedis for amino acid analysis, Ram Seetharam for N-terminal amino acid sequencing, and Barbara Larsen for electrospray mass spectrometry analysis. R.F. and S.J.A.-C. acknowledge postdoctoral research support from National Institutes of Health Grants GM14321 and GM13731.

1. Benezra, R., Davis, R. L., Lockshon, D., Turner, D. L. & Weintraub, H. (1990) *Cell* **61,** 49–59.
2. Jones, N. (1990) *Cell* **61,** 9–11.
3. Peterson, C. A. (1991) *New Biol.* **3,** 442–445.
4. Lamb, P. & McKnight, S. L. (1991) *Trends Biochem. Sci.* **16,** 417–422.
5. Blackwood, E. M. & Eisenman, R. N. (1991) *Science* **251,** 1211–1217.
6. Murre, C., McCaw, P. S. & Baltimore, D. (1989) *Cell* **56,** 777–783.
7. Davis, R. L., Cheng, P.-F., Lassar, A. B. & Weintraub, H. (1990) *Cell* **60,** 733–746.
8. Anthony-Cahill, S. J., Benfield, P. A., Fairman, R., Wasserman, Z. R., Brenner, S. L., Altenbach, C., Hubbell, W. L., Stafford, W. F., III, & DeGrado, W. F. (1992) *Science* **255,** 979–983.
9. Halazonetis, T. D. & Kandil, A. N. (1992) *Science* **255,** 464–466.
10. Vinson, C. R. & Garcia, K. C. (1992) *New Biol.* **4,** 396–403.
11. Ferre-D'Amare, A. R., Prendergast, G. C., Ziff, E. B. & Burley, S. K. (1993) *Nature (London)* **363,** 38–45.
12. Lassar, A. B., Davis, R. L., Wright, W. E., Kadesch, T., Murre, C., Voronova, A., Baltimore, D. & Weintraub, H. (1991) *Cell* **66,** 305–315.
13. Murre, C., McCaw, P. S., Vaessin, H., Caudy, M., Jan, L. Y., Jan, Y. N., Cabrera, C. V., Buskin, J. N., Hauschka, S. D., Lassar, A. B., Weintraub, H. & Baltimore, D. (1989) *Cell* **58,** 537–544.
14. Sun, X.-H., Copeland, N. G., Jenkins, N. A. & Baltimore, D. (1991) *Mol. Cell. Biol.* **11,** 5603–5611.
15. Christy, B. A., Sanders, L. K., Lau, L. F., Copeland, N. G., Jenkins, N. A. & Nathans, D. (1991) *Proc. Natl. Acad. Sci. USA* **88,** 1815–1819.
16. Biggs, J., Murphy, E. V. & Israel, M. A. (1992) *Proc. Natl. Acad. Sci. USA* **89,** 1512–1516.
17. Ellis, H. M., Spann, D. R. & Posakony, J. W. (1990) *Cell* **61,** 27–38.
18. Garrell, J. & Modolell, J. (1990) *Cell* **61,** 39–48.
19. Farmer, K., Catala, F. & Wright, W. E. (1992) *J. Biol. Chem.* **267,** 5631–5636.
20. Brandts, J. F. & Kaplan, L. J. (1973) *Biochemistry* **12,** 2011–2024.
21. Buskin, J. N. & Hauschka, S. D. (1989) *Mol. Cell. Biol.* **9,** 2627–2640.
22. Knott, G. D. (1979) *Comput. Programs Biomed.* **10,** 271–280.
23. Wong, I., Chao, K. L., Bujalowski, W. & Lohman, T. M. (1992) *J. Biol. Chem.* **267,** 7596–7610.
24. Liu, S. & Stafford, W. F. (1992) *Biophys. J.* **61,** A476 (abstr.).
25. Ansevin, A. T., Roark, D. E. & Yphantis, D. A. (1970) *Anal. Biochem.* **34,** 237–261.
26. Brenner, S. L., Zlotnick, A. & Stafford, W. F. (1990) *J. Mol. Biol.* **216,** 949–964.
27. O'Shea, E. K., Rutkowski, R., Stafford, W. F. & Kim, P. S. (1989) *Science* **245,** 646–648.
28. Laue, T. M., Klevit, R. E., Starovasnik, M. A. & Weintraub, H. (1992) *Biophys. J.* **61,** A476 (abstr.).
29. Starovasnik, M. A., Blackwell, T. K., Laue, T. M., Weintraub, H. & Klevit, R. C. (1992) *Biochemistry* **31,** 9891–9903.
30. Sun, X.-H. & Baltimore, D. (1991) *Cell* **64,** 459–470.
31. Fisher, D. E., Carr, C. S., Parent, L. A. & Sharp, P. A. (1991) *Genes Dev.* **5,** 2342–2352.
32. Pesce, S. & Benezra, R., *Mol. Cell. Biol.*, in press.